ORNL/TM-2021/2312

Oak Ridge National Laboratory Fission Product Hydrochlorination

Joanna McFarlane
Trent Walker

November 2021

ORNL IS MANAGED BY UT-BATTELLE LLC FOR THE US DEPARTMENT OF ENERGY

DOCUMENT AVAILABILITY

Reports produced after January 1, 1996, are generally available free via US Department of Energy (DOE) SciTech Connect.

Website www.osti.gov

Reports produced before January 1, 1996, may be purchased by members of the public from the following source:

National Technical Information Service
5285 Port Royal Road
Springfield, VA 22161
Telephone 703-605-6000 (1-800-553-6847)
TDD 703-487-4639
Fax 703-605-6900
E-mail info@ntis.gov
Website http://classic.ntis.gov/

Reports are available to DOE employees, DOE contractors, Energy Technology Data Exchange representatives, and International Nuclear Information System representatives from the following source:

Office of Scientific and Technical Information
PO Box 62
Oak Ridge, TN 37831
Telephone 865-576-8401
Fax 865-576-5728
E-mail reports@osti.gov
Website http://www.osti.gov/

This report was prepared as an account of work sponsored by an agency of the United States Government. Neither the United States Government nor any agency thereof, nor any of their employees, makes any warranty, express or implied, or assumes any legal liability or responsibility for the accuracy, completeness, or usefulness of any information, apparatus, product, or process disclosed, or represents that its use would not infringe privately owned rights. Reference herein to any specific commercial product, process, or service by trade name, trademark, manufacturer, or otherwise, does not necessarily constitute or imply its endorsement, recommendation, or favoring by the United States Government or any agency thereof. The views and opinions of authors expressed herein do not necessarily state or reflect those of the United States Government or any agency thereof.

ORNL/TM-2021/2312

Nuclear Energy and Fuel Cycle Division

OAK RIDGE NATIONAL LABORATORY FISSION PRODUCT HYDROCHLORINATION

Joanna McFarlane
Trent Walker

November 2021

Prepared by
OAK RIDGE NATIONAL LABORATORY
Oak Ridge, TN 37831-6283
managed by
UT-BATTELLE, LLC
for the
US DEPARTMENT OF ENERGY
under contract DE-AC05-00OR22725

CONTENTS

LIST OF FIGURES

LIST OF TABLES

ABBREVIATIONS

DI	deionized
DOE	US Department of Energy
FP	fission product
ICP-MS	inductively coupled plasma mass spectrometry
ID	inner diameter
INL	Idaho National Laboratory
KOP	knock-out pot
HALEU	high assay low enrichment uranium
MRPP	Material recovery pilot plant
ORNL	Oak Ridge National Laboratory
PFA	perfluoroalkoxy
XRF	x-ray fluorescence
ZIRCEX	zirconium extraction

EXECUTIVE SUMMARY

This work supports the recovery of high-assay low-enriched uranium (HALEU, uranium enriched in ^{235}U to >5% and <20%) from used nuclear fuel through a process based on the zirconium extraction (ZIRCEX) process. The ZIRCEX process starts with the dry head-end removal of zirconium or aluminum cladding from the nuclear fuel via chlorination or hydrochlorination, which results in the separation of cladding from the fuel as the metal chloride (e.g., aluminum trichloride or zirconium tetrachloride). The hydrochlorination process is included in the Material Recovery Pilot Plant (MRPP), a ZIRCEX-based demonstration plant at Idaho National Laboratory (INL). The experiments outlined in this report assessed fission product (FP) volatility and transport under the hydrochlorination conditions used to separate cladding from used nuclear fuel.

The scope of the experiments reported here was based on consultation with INL and comprises a set of parametric studies based on the goal of successfully operating the hydrochlorination process at a relatively low temperature to minimize losses of uranium from the reactor.

This set of experiments used a variety of simulated fissions products, as well as fuel cladding, that would be expected to be significant constituents present in spent metallic fuel. Although in actual spent metallic fuels these fissions products would be expected to exist primarily as metals, for the scope of this project some chlorides were used to obtain a general idea of the expected behaviors of these materials under the conditions typically used for hydrochlorination. If material volatilization occurs, more in-depth experiments will be conducted by using more realistic surrogate material. These were small-scale experiments that used a quartz hydrochlorination reactor with an inner diameter of 2.5 cm and a length of 38 cm rather than the larger-scale system described in the earlier reports (Del Cul and Hunt 2019, McFarlane et al. 2020, McFarlane et al. 2021). The furnace had three heating zones that were a combined 30.5 cm in length to accommodate most of the reaction vessel. The reactor was linked to a knock-out pot (KOP) for elutriated powders and fumes, which in turn was linked to a deionized (DI) water scrubber to capture unreacted HCl and any FP fumes that bypassed the KOP.

In these tests, a mixture of simulated FPs was added to a fluidized bed of SiO_2. The powders included Mo, $SrCl_2$, Sn, CsI, CsCl, Te, and $LaCl_3$ to cover a wide range of FP types. The only oxide used was SiO_2. Three tests were performed by using the same mixture of FPs, with the only difference being the addition of aluminum and zirconium cladding in the second and third tests, respectively. The goal was to simulate any possible reaction of FPs with cladding material during hydrochlorination. Uranium was not added to the mixture as the focus was on FP that could have escaped the fuel during chemical decladding.

The first and third tests were performed at 350°C, and the second test was performed at 200°C. The mixture was preheated to the desired temperature under a flow of argon, and once this temperature was reached, the argon was replaced by HCl(g) that flowed into the bed from a gas cylinder for 30 min. The amount of HCl that passed through the bed was determined by using results from online conductivity measurements in the scrubber located after the reaction vessel. Other measurements included temperatures from the furnace controller.

After each test, the apparatus was taken apart and the solids collected. Gravimetry was used to determine the fraction of materials removed from the SiO_2, and apparatus components were rinsed with DI water. The slurries and powders were examined by x-ray fluorescence (XRF), and the samples were sent for metals analysis via inductively coupled plasma mass spectrometry measurements (ICP-MS).

XRF measurements qualitatively indicated that most of the powder transported from the bed was elutriated as a molybdenum species, which was introduced as a fine powder into the mixture. The elutriation occurred under the flow of argon before HCl(g) was introduced into the system.

ABSTRACT

This work supports the recovery of high-assay low-enriched uranium (HALEU, uranium enriched in ^{235}U to >5% and <20%) from used nuclear fuel through a process based on the zirconium extraction (ZIRCEX) process. Part of the process involves removing the cladding via hydrochlorination at temperatures that are thermodynamically favored for chlorination of the cladding but not the fuel. This work describes the outcome of key fission products (FPs) during the hydrochlorination process. These tests were a scoping study and thus used surrogates and not actual radiological material. Three tests were performed to investigate the volatility and transport of FP simulants in a hydrochlorination reactor. The simulants were chosen to represent the main classes of semi- and nonvolatile FPs in abundances typical of high-burnup fuel. The FP volatilities were tested in flows of HCl(g) at 200 and 350°C in the presence of aluminum and zirconium, respectively. The results indicate that enhanced transport was observed for Sn, Sr, Mo, and Te in the presence of the cladding materials. These scoping experiments will help to assess a need for further tests that investigate FP reaction, vaporization, and transport from the fluidized bed reactor.

1. INTRODUCTION

Research into nuclear reprocessing began in the 1960s as a way to recover uranium and plutonium from spent nuclear fuel (SNF) to be recycled into future reactors, which increases energy utilization. Due to the political climate at the time and rapidly increasing proliferation concerns, research into reprocessing methods dwindled and was ultimately banned by the Carter Administration in 1977 (Martinez 2002). Because advanced Generation IV reactor designs require more highly enriched uranium fuels—as compared to the current 3-5% used in light water reactors—the US Department of Energy (DOE) is considering short-term solutions to address shortages of these fuels. One of these strategies is to recycle highly enriched SNF from government-owned research reactors and down-blend it into HALEU fuel with the desired isotopic ratio. One method to accomplishing this would be to utilize a hybrid ZIRCEX process, which involves using a hydrochlorination step to volatilize the zirconium/aluminum cladding and separate it from the nonvolatile UCl_3. The uranium would then be passed through a typical solvent extraction-based reprocessing flow sheet, such as PUREX, UREX, or another separation scheme, such as fluoride volatility, to separate the uranium from its fission products before being down-blended and ultimately returned to metal/oxide form for use in future reactors.

The use of halogenation to separate aluminum and zirconium cladding from metallic uranium has been under consideration since the 1960s. Argonne National Laboratory staff performed hydrochlorination experiments on aluminum- and zirconium-clad uranium fuels (Lawroski et al., 1963, 1967). Volatile Al_2Cl_6 and $ZrCl_4$ were removed from the fuel, whereas nonvolatile uranium remained in a 28–100 mesh fluidized alumina bed. Based on the results of these earlier studies, DOE commissioned the Material Recovery Pilot Plant, which declads metallic uranium fuel via hydrochlorination. To facilitate the development of the ZIRCEX process, ORNL focused on how different processing parameters affect the kinetics and separation of uranium from cladding material. ORNL staff conducted laboratory-scale parametric tests to determine the optimal bed volume, HCl(g) flow rate, and reaction temperatures (Del Cul and Hunt Cul 2019, McFarlane et al. 2020). The possible reaction of uranium was investigated and found to be minimal (McFarlane et al. 2020, 2021). The current report delves into the outcome of various FPs and examines how different FPs are expected to partition throughout the system. This work will help to determine what subsequent steps need to be taken to successfully separate the useful fuel material from the waste and what mitigation needs to be implemented to prevent volatile FP spreading throughout the process.

2. EXPERIMENTAL

In these tests, a mixture of simulated FPs was added to a fluidized bed of SiO_2. The powders included Mo, $SrCl_2$, Sn, CsI, CsCl, Te, and $LaCl_3$ to cover a wide range of FP types. In metallic fuels, FPs are not expected to start as chlorides and should remain the in the fuel matrix during chemical decladding. These tests were designed to evaluate the possibility of transport should degradation of the matrix itself allow for FP reaction. If FP chlorides appear to be volatile, then experiments that more accurately represent spent metallic simulated high-burnup nuclear fuel will be proposed. Thus, in the beginning, the materials were chlorides or metals. The only oxide used was SiO_2. Three tests were performed by using the same mixture of FPs, but the second and third tests included added aluminum 6061 and zircaloy-4, respectively, to simulate the chemical reactions of the cladding materials.

2.1 MATERIALS AND FISSION PRODUCT SIMULANT PREPARATION

Most of the simulated FPs used for this experiment were on hand from previous experiments. Lanthanum Chloride (99.9%) was obtained from J.T. Baker Inc. Cesium chloride (99.999% metals basis) was obtained from Alfa Aesar. Suprapur^{TM} Cesium iodide was obtained from Millipore Sigma. Tellurium metal was obtained from Fisher Scientific. Tin powder (<150um, 99.5% trace metals basis) and olybdenum powder (1-5um, 99.9% trace metals basis) were obtained fresh for this experiment from Sigma-Aldrich.

Anhydrous HCl gas (99%) was obtained from Air Liquide. Reactor grade claddings—aluminum 6061 and zircaloy-4—were obtained from McMaster-Carr and Westinghouse, respectively. SiO_2 was obtained from Sigma-Aldrich and was sieved to 90-125 µm particle size. The 60-mesh bed material was the standard size used for the earlier hydrochlorination experiments.

The ratio of each FP species present in the starting sample matrix (Table 1) was representative of what would be expected to be present in an actual spent fuel sample based on Origin run calculations for spent nuclear fuel with a burnup of 40 GWd/MTHM and cooled for 10 years.

Table 1. Matrix composition.

Materials	**Mass added (g)**		
	Test 1	**Test 2**	**Test 3**
CsCl	0.925	0.918	1.073
CsI	0.137	0.138	0.163
Mo	1.12	1.12	1.292
Sn	0.01	0.138	0.017
Te	0.15	0.138	0.19
$LaCl_3$	0.725	0.725	0.839
$SrCl_2$	N/A	0.722	0.85
Zr	N/A	N/A	1.291
Al	N/A	1.253	N/A

The experiments started by weighing out the required amount of each material for the respective run and combining them—minus the Zr and Al metal, where applicable. Because water vapor was observed in the reactor during Test 1, the $LaCl_3$ and $SrCl_2$ were dried in a vacuum oven overnight before Tests 2 and 3 to obtain a more accurate mass balance. Then, the powder mixture was ground with a mortar and pestle before being combined with the SiO_2 bed material and homogenized by stirring. For runs that used fuel cladding, the metal cladding was cut into small pieces (~0.2–0.4 g) and combined with the ground FPs and bed material before being added to the reactor. The SiO_2 bed material was ground, sieved to a 90–125 µm nominal size, and dried before being used in experiments.

2.2 APPARATUS

Small-scale experiments were conducted that used a quartz hydrochlorination reactor rather than the larger-scale system described in the earlier reports (DelCul and Hunt 2019; McFarlane et al. 2020; McFarlane et al. 2021). ORNL's glass shop designed and manufactured two glass vessels. The first vessel was used as the reaction vessel for the tests; it had a 3.81 cm inner diameter (ID), was 25.4 cm long, and had a 5 µm glass frit toward the bottom of the apparatus. The second vessel was used as a knock-out pot (KOP); it had a 6.35 cm ID and was 38 cm long. The dimensional ratio of the quartz reactor to the stainless-steel reactor used in earlier hydrochlorination experiments was 0.43. A schematic of the apparatus is shown in Figure 1.

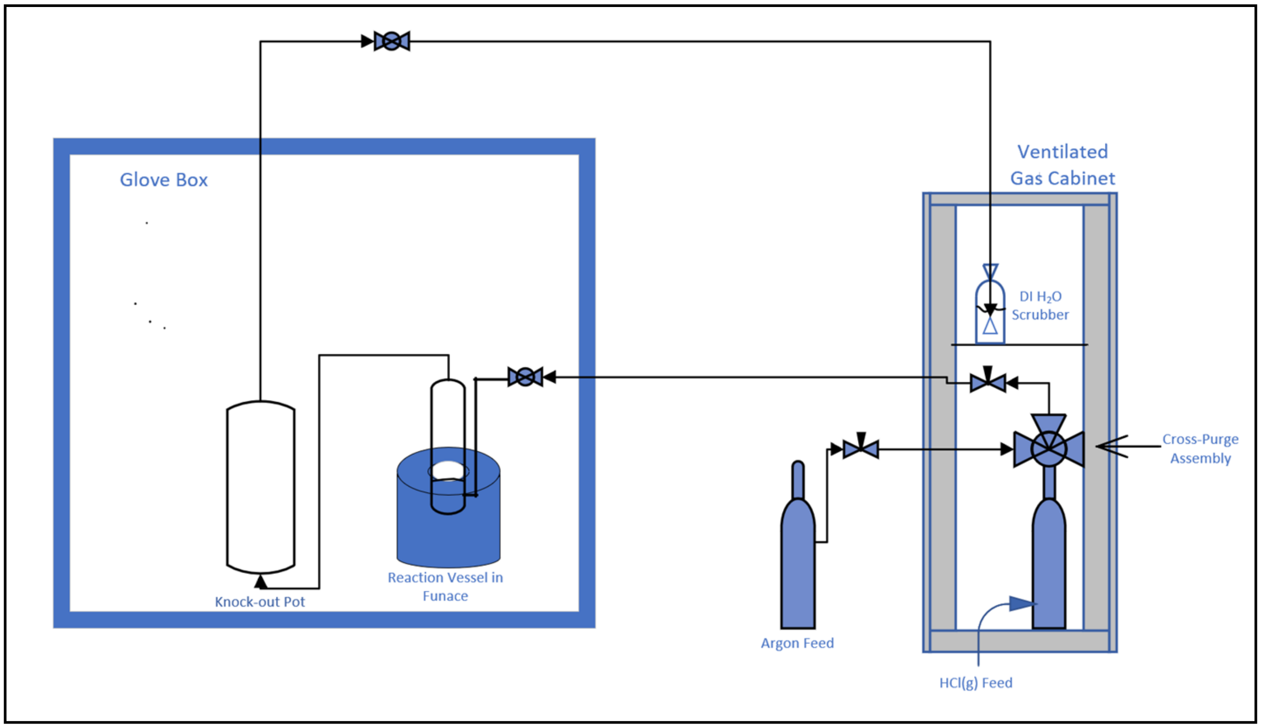

Figure 1. Annotated schematic of the hydrochlorination apparatus.

The furnace had three heating zones that were 30.5 cm long to accommodate most of the reaction vessel. The reactor was linked to a KOP for elutriated powders and fumes, which in turn was linked to a deionized (DI) water scrubber to capture unreacted HCl and any FP fumes not captured by the KOP.

A conductivity meter located in the scrubber solution was used to monitor the flow of HCl(g) as it exited the reaction vessel and dissolved in the scrubber. The conductivity meter was calibrated by using a series of HCl(aq) solutions of differing volumetric ratios that covered a dynamic range of two orders of magnitude. The amount of HCl that passed through the bed over the complete test was calculated based on the resulting conductivity measurements in the scrubber at the end of the experiment. This value was corrected by the losses incurred due to the chlorination of FP simulants. Other measurements included temperatures from the furnace controller.

2.3 CALIBRATION OF HCl MEASUREMENT

The amount of HCl(g) going through the scrubber was monitored continuously via a conductivity probe located in the scrubber. The probe was calibrated by using reagent HCl (Fisher 6 N, Lot 131601). The stock was diluted to 3.5, 0.35, and 0.035 vol %. The conductivity meter provided two measurements: micro siemens per centimeter and parts per million, the latter derived from the former. The conductivity measurements were fit to a linear regression that was used to analyze the scrubber solutions during and after the experiments, as shown in Figure 2.

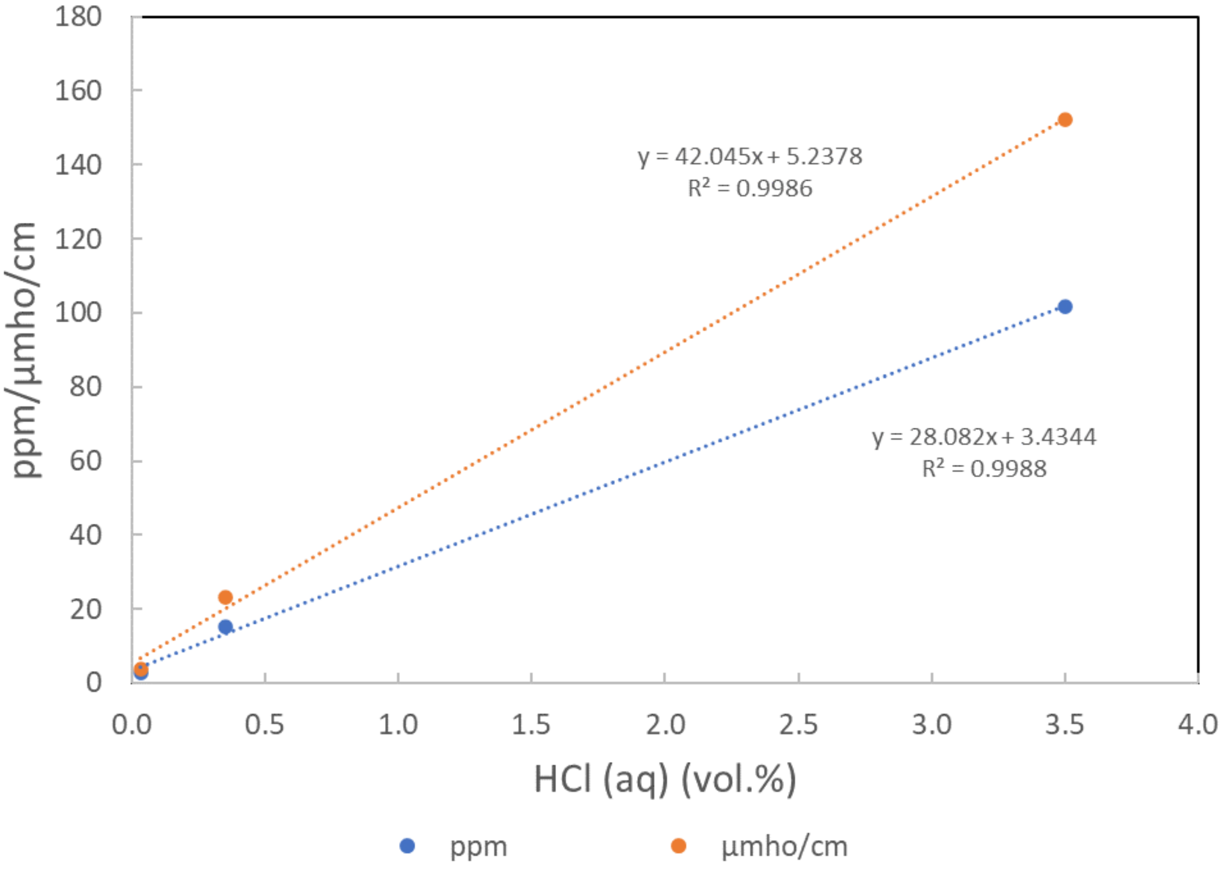

Figure 2. Calibration of conductivity meter for HCl(aq) concentration.

2.4 EXPERIMENTAL METHOD

The first and third tests were performed at 350°C, and the second test was performed at 200°C. During tests, the bed was preheated to the desired temperature under a flow of argon, and once this temperature was reached, the argon was replaced by HCl(g) that flowed into the bed from a gas cylinder for 30 min.

At the end of the experiment, the apparatus was flushed with argon and left to cool overnight before it was dismantled. The pieces that were disassembled and checked included the reactor, the top of the reactor, the tubing from the reactor to the KOP, the KOP, and the scrubber. Powder from each component was collected dry, and the components were rinsed. Samples of the powders and rinses were analyzed by inductively coupled plasma mass spectrometry (ICP-MS) and x-ray fluorescence (XRF).

All samples that were sent off for XRF were analyzed as received. For ICP-MS analysis, all samples were dissolved in a mixture of 2-4 M HNO_3, 1 M HCl, and trace HF (~1%). Some of the solids in the ICP-MS samples did not fully dissolve and small amounts of brick-red or white solids were observed falling out of solution over time. These samples were filtered to get a mass of the undissolved solids and then digested in an oven.

2.4.1 TEST 1: NO CLADDING EXPERIMENTAL CONDITIONS

The first test was performed at 350°C without cladding material to set a baseline on how fission products would be expected to behave sans cladding or uranium. The mixture was preheated to 350°C under a flow of argon. During this time, H_2O was observed condensing in the top of the reaction vessel, and yellow vapor was seen in the KOP. The yellow vapor eventually dissipated and a small amount of metallic silver needles in the bottom of the KOP was observed as seen in Figure 6.

The uptake of HCl(g) into the scrubber is shown in Figure 3. The scrubber concentration increased significantly at 20 min as the needle valve into the cylinder was opened. With HCl(g) flowing, a black powder appeared at the top of the reactor, and a pink cloud formed in the KOP as seen in Figures 7 and 8, respectively. As the flow continued, a black residue also appeared in the KOP. At 30 min, the HCl(g) flow was stopped, and an argon purge was started.

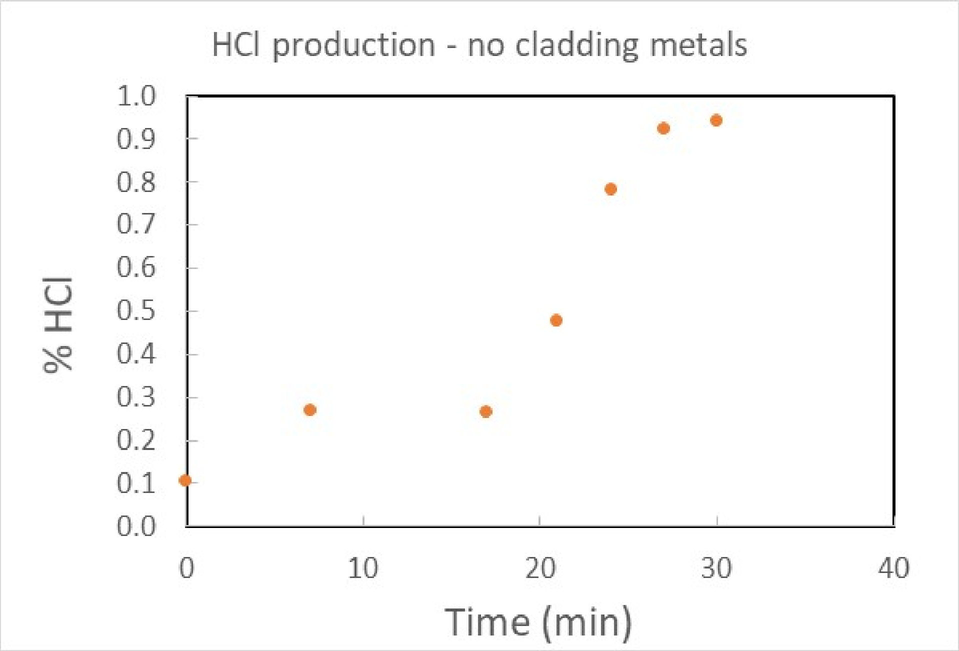

Figure 3. Concentration of HCl(aq) in the water scrubber as a function of time for Test 1.

2.4.2 TEST 2: ALUMINUM CLADDING EXPERIMENTAL CONDITIONS

The operating temperature for the second test was 200°C with aluminum alloy 6061 added to the mixture of FP simulants. The mixture was preheated under a flow of argon, and once the desired temperature was reached, the argon was replaced by HCl(g) that flowed into the bed from a gas cylinder for 30 min. During preheating, black powder was seen being transported from the reactor before the HCl(g) was added. Once the HCl(g) was introduced to the system, the presence of a reaction was immediately seen via the formation of a white-yellow fume. This was accompanied by a temperature rise in the center of the furnace from 200 to 227°C. The formation of the pink-colored fume, yellow vapor, and silver needles seen in the first test were not seen during this test. The results in Figure 4 show the HCl uptake in the scrubber leveled off 10 minutes before the HCl(g) flow was stopped.

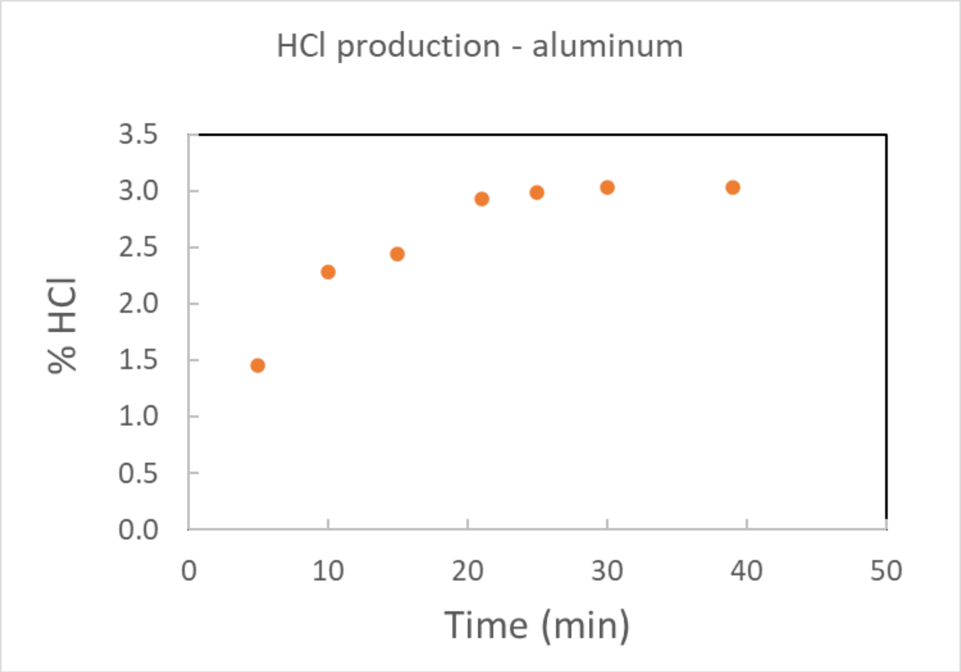

Figure 4. Concentration of HCl(aq) in the water scrubber as a function of time for Test 2.

2.4.3 TEST 3: ZIRCALOY CLADDING EXPERIMENTAL CONDITIONS

The third mixture was preheated to 350°C under a flow of argon. When the desired temperature was reached, the argon was replaced by HCl(g) that flowed into the bed from a gas cylinder for 30 min. The flow of HCl was monitored by uptake into the aqueous scrubber, as shown in Figure 5.

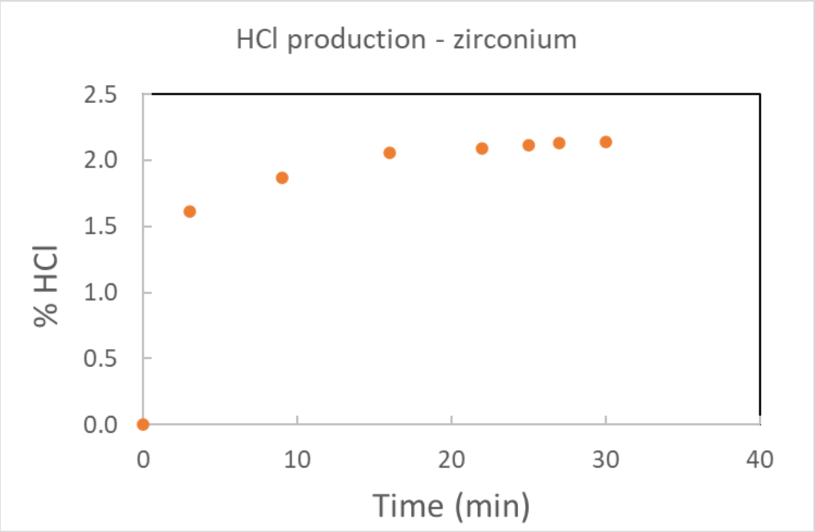

Figure 5. Concentration of HCl(aq) in the water scrubber as a function of time for Test 3.

When the flow of HCl(g) was started, a white cloud immediately formed and was transported to the KOP, where it settled. The fine white powder also settled in the line exiting the KOP. This was the only test in which powder was visibly transported beyond the KOP. The scrubber solution became yellow, and the percentage of HCl rose rapidly to 1.6 vol % in the first 2 min of the experiment. The temperature of the reactor rose to 357°C in the first 5 min of the test but stabilized afterward. At about 24 min, the line to the scrubber appeared to be blocked as bubbles were no longer visible in the scrubber. The HCl(g) was turned off, and an argon purge was started at 31 min. The additional gas pressure caused solids to emerge from the perfluoroalkoxy (PFA) fitting at the top of the KOP, indicating that the line from the KOP had become clogged with solids. The gas flow was immediately shut off. The apparatus was left to cool, and sampling occurred the following day.

3. RESULTS

After each test, the apparatus was taken apart and the solids were collected. Gravimetry was used to determine the fraction of materials removed from the SiO_2 bed. The apparatus components were rinsed with DI water to remove any residual powder adhered to the walls of the apparatus. The slurries and powders were examined by XRF, and the samples were sent for ICP-MS measurements for metals analysis. Results are presented in Table 2.

Table 2. Percentage of FP simulant transferred during hydrochlorination.

Element	Test 1: 350°C	Test 2: 200°C, added Al	Test 3: 350°C, added Zr
Cs	0.18±0.04	4.9±1.0	3.4±0.7
Te	1.3±0.3	7±1	26±5
Mo	1.2±0.2	56±11	42±8
Sn	21±4	39±8	109±22
Cladding	N/A	9 (Al) ±2	44 (Zr) ±9
La	0.04±0.01	0.8±0.2	2.1±0.4
Sr	0.45±0.08	11±2	9±2
I	27±5	28±6	24±5

Uncertainty in the measurement comes from mass losses during sampling of the KOP and tubing and other parts of the apparatus (±10%) as well as the analysis (±10%). It should be noted that all visual observations regarding the color of materials seen during the experiments discussed within this paper are subjective. They were viewed through the Lucite™ panels of the glove box under fluorescent light.

3.1 TEST 1: NO CLADDING

The first test was conducted without the presence of cladding material to determine a baseline of how different FPs would be expected to behave under these conditions. During the heating phase—before initiating the HCl(g) flow—two notable observations were made. First, water vapor was seen condensing at the top of the reactor due to the gas cooling as it exited the heating zone. This indicated that some of the starting material—namely the lanthanum and strontium chlorides—were hydrated, which is a potential source of error for Test 1. This could also have the negative consequence of the steam reacting with the starting materials to form compounds that would not normally be seen in this process. The second notable observation was the presence of yellow vapor in the KOP during heating, as seen in Figure 6, which indicated that components in the starting material reacted each other—or with the water liberated from the hydrated La and Sr. The latter explanation may be more likely since the yellow vapor was not seen in the subsequent tests when the La and Sr were dried prior to being mixed with the bed compounds. Identification of the yellow compound is difficult, since it was not isolated to be analyzed prior to addition of more material during the chlorination step. However, the identity of this material should be a non-factor in full scale operation since it only forms in the presence of water—and was not seen in subsequent steps.

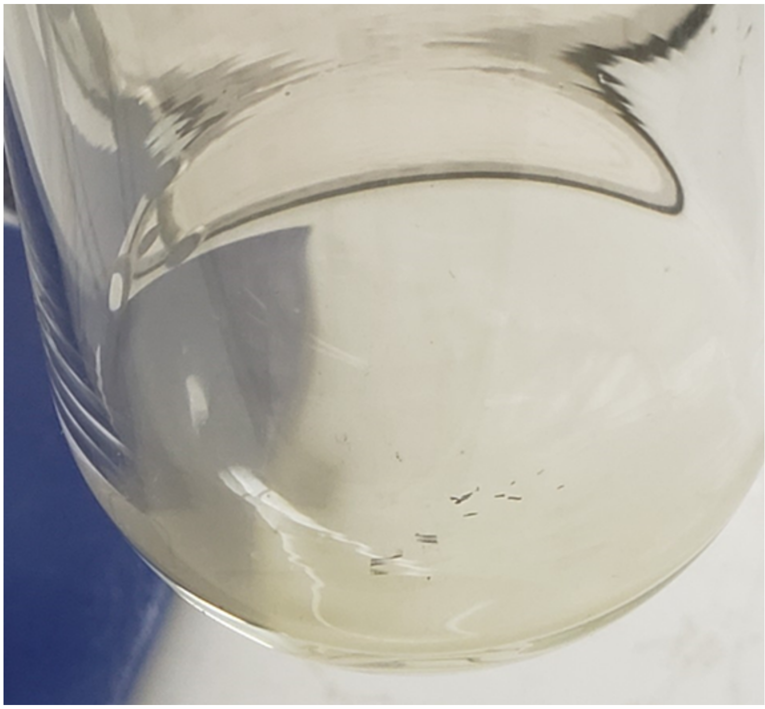

Figure 6. Yellow vapor and silver solids in KOP during Test 1 Preheating

Once HCl flow was started, the transport of material out of the bed was immediately evident by the presence of black powder at the top of the reaction vessel (Figure 7) and pink powder in the KOP (Figure 8). Both materials are thought to be compounds of molybdenum, which is supported by XRF (Figures B3 and B4) and ICP-MS data (Table A1) showing the primary constituents of those two samples to be molybdenum. The chemical form of these species is unknown, since no molecular analysis was done to determine this; however, the black powder is thought to be small particles of unreacted molybdenum that was mobilized by the gas stream. Elutriation of less dense and small sized powders could have been possible. The pink powder is thought to be an oxychloride or chloride of molybdenum—perhaps $MoCl_3$ or $Mo_2O_3Cl_6$ due to the color of the powder and reactants present during the reaction. Both the black and pink materials seen during this experiment were in small quantities, and overall, a majority of the material stayed in the bed.

ICP-MS results for this experiment suggest that less than 2 wt.% of the starting material exited the bed for Cs, Te, Mo, La, and Sr on a metals basis. However, I and Sn showed greater tendency to transport with 26 and 21 wt.% metal, respectively. The iodine and tin compounds exiting the bed primarily ended up in the scrubber.

Figure 7. Black powder in reactor top after HCl(g) introduction in Test 1

Figure 8. Pink powder in KOP after HCl(g) introduction in Test 1

3.2 TEST 2: ALUMINUM CLADDING

For this experiment, pieces of a 6061-alloy aluminum coupon were added to the SiO_2 bed to determine the effect of Al_2Cl_6 vapor formation on the volatility of FP simulants. The test was conducted at 200°C, which is the temperature at which aluminum chloride can form and become volatile. There were several notable differences between this run and the first run conducted without aluminum cladding. The first difference was that no water vapor was seen condensing at the top of the reactor, which stemmed from the change in sample preparation made between Tests 1 and 2—drying of the $LaCl_3$ and $SrCl_2$ salts prior to the experiment. This change was made to achieve a more accurate mass balance for Sr and La, as well as to prevent any undesired reactions occurring due to the presence of water vapor. Another notable difference was that no yellow vapor was seen in the KOP during heating; however, there was some transport of a black/gray powder as seen in Figure 9.

Figure 9. Black/gray powder in KOP during Test 2 Preheating

The transport of this material during heating reinforces the likelihood that the material in the first test was fluidized Mo metal because no reactions should be occurring in the bed during heating without the presence of water vapor. Once the HCl(g) flow commenced, a white cloud of a semi-volatile compound—likely tin chloride (Sn(II) or Sn(IV)) and Al_2Cl_6—was seen exiting the reactor and being deposited throughout the system as seen in Figure 10. For this experiment, Sn, Mo, Sr and I saw a significant degree of transport, with 39, 56, 11 and 28 wt.% (metals basis) being transported out of the bed, respectively. The other constituents mostly stayed in the bed. The tin was likely transported as semi-volatile $SnCl_4$, which then deposited downstream of the reactor as it cooled. Meanwhile, the Mo was likely transported as a metal powder via physical means. The strontium saw much greater transport during this experiment compared to the first test, with a 24-fold increase in material transport out of the bed. This increase in transport was likely caused by the strontium forming an adduct with the aluminum chloride. This is supported by the ICP-MS analysis which shows that strontium mainly deposited in the transfer line, while aluminum chloride mainly deposited in the transfer line and top of the reactor. Overall, only 9.2% of the aluminum was transferred from the bed. Possible reasons for the limited transport of aluminum include not allowing enough time for complete reaction of the material, insufficient flow rate of HCl to fluidize the bed—thus decreasing available surface area for reaction, or possible analytical issues. This indicates that our experimental setup likely needs to be improved in order to get more representative results of how cladding volatility impacts the behavior of fission products in the system.

Figure 10. White powder in reactor top after HCl(g) introduction in Test 2

3.3 TEST 3: ZIRCALOY CLADDING

Small pieces of zircaloy-4 cladding were added to the SiO_2 bed so that the effect of $ZrCl_4$ vapor formation on the volatility of FP simulants could be observed. The test was conducted at 350°C, which is the temperature at which zirconium tetrachloride can form and become volatile. Unlike in previous tests, no material was seen exiting the bed during the preheating phase of the experiment; however, visible reaction occurred immediately after HCl(g) was introduced into the system. Although the reactor remained the black/gray color typical of Mo, the KOP, the top of the reactor, and the PFA line exiting the KOP became a tan-white color as powder was deposited on their surfaces. This was likely due to the formation of $ZrCl_4$, which then sublimed at 331°C and was carried out of the reactor in the gas phase before depositing on the walls of the system as it cooled downstream. Because of the physical properties of the compound, it is unlikely that the $ZrCl_4$ was transported past the KOP as a gas and more likely condensed and deposited as a fine powder (fume or aerosol) that was transported by physical means. In this test, there was a much greater transport of material out of the bed than in the other two tests; Te, Mo, Sn, Zr, and I were transported out of the bed to large degrees. Most of this material was then deposited in the first transfer line and KOP; however, it is possible that this was caused by plugging of the line and suspension of flow rather than by the material naturally depositing in these parts of the system. Another unique occurrence during this test was the change in scrubber solution color from clear to yellow, which was caused by the formation of $ZrOCl_2$ in the scrubber.

4. DISCUSSION

The amount of FP simulant transport was compared between three hydrochlorination tests. The results indicated that certain compounds were removed from the bed from either the flow of gas or reaction with HCl(g). For other species, the volatility was minimal. The removal of FP simulants from the bed for the three tests is compared in Table 2.

The tests indicate that the transport of tin and iodine was substantial for each test, with both mainly being deposited in the scrubber. The iodine was unaffected by the presence of the other constituents of the system or the temperature, suggesting that the chemical form was volatile even at 200°C, perhaps as HI or I_2. The tin became more volatile with the addition of the metals, so there may have been some association between the tin and Al_2Cl_6 or $ZrCl_4$. As expected, both cladding metals were fairly volatile as the hydrochlorination conditions were established to strip off these metals, and the percentage of Zr transported was higher than that of Al. However, the kinetics of this process were not studied explicitly. Substantial amounts of molybdenum were transported in both the tests with added cladding material. The molybdenum did not transfer past the KOP; however, and so it may have been associated with the volatile cladding material. Tellurium saw increases in volatility with the presence of the cladding materials, 5.5 times with aluminum and 20 times with zirconium. Tellurium behavior is complex; most of the tellurium moved to the scrubber in the second test, and most was moved to the KOP in the third test. Strontium relocation was also enhanced in the presence of cladding materials.

Unlike iodine, most of the cesium was found in the reactor. The lanthanum also appeared to be less likely to move from the reactor itself, although all of these saw increased relocation when the cladding materials were added to the bed. All of these chlorides are nonvolatile under the conditions of the experiment and thus were unlikely to have been vaporized from the fluidized bed.

These results indicate that some FPs could become volatile during hydrochlorination, even under conditions that might be considered fairly mild. Iodine will likely be removed from spent fuel along with fission gases, and thus can be trapped before the hydrochlorination process. Stable nonvolatile chlorides will remain in the fluidized bed, although a certain fraction will evolve, perhaps in association with other volatile components. Tin, molybdenum, and tellurium are greatly affected by the presence of the cladding materials, and further study is recommended.

5. IMPROVEMENTS FOR FUTURE EXPERIMENTS

There are several improvements that could be implemented in this experiment to improve the quantity and quality of data received in future experiments.

- The first improvement would be the sieving of all powders to a consistent particle size prior to reaction. The uncertainty in particle size distribution for the samples made it difficult to determine whether materials were transported out of the bed due to entrainment in the gas stream versus leaving the bed due to chemical change such as adduct formation or reacting to form a volatile species.
- Another improvement that could be made for this experiment is using larger masses of fission products. Due to the low quantity of some material added to the system, in conjunction with the difficulty in quantitatively removing the powder from the system, small losses of material resulted in large errors propagating through our calculations. This was also the case for some of the analytical results where detection of some species was close to detection limit for dilute samples.
- Another notable problem with this experiment was the absence of an accurate, quantitative method for determining gas flow through the system. Due to the corrosion of HCl mass flow controller that was set aside for this experiment, flow rate determination was done using visual methods in conjunction with back-calculations, which have less resolution than direct

measurement). This could have two negative consequences. First, since linear velocity influences fluidization of the particles, it is difficult to say definitively that the differences in material transport between runs was solely caused by the presences—or lack thereof—of cladding material. It is possible that the flow rates were not consistent between runs, and that the differences in elutriated materials between runs is partially due to changes in the amount of material fluidized due to changes in gas flow rate. The second negative consequence of this is providing different amounts of reactants between tests.

- The final improvement that can be made, would be the implementation of a device capable of determining speciation of materials. This could be done via an online method for monitoring of the gas stream leaving the reactor and the scrubber—such as Fourier Transform Infrared Spectroscopy—or using a method such as powder XRD to determine the composition post run. This would help in determining in what form fission products leave the reactor in addition to ascertaining when the reaction has been completed. Additionally, implementing online analysis downstream of the scrubber would allow us to verify that all materials are being captured by the KOP or scrubber. This would help to ensure a more complete mass balance.

6. CONCLUSIONS

Three tests were performed to investigate the volatility and transport of FP simulants in a hydrochlorination reactor. The simulants were chosen to represent the major classes of semi- and nonvolatile FPs in abundances typical of high-burnup fuel. The FP volatilities were tested in flows of HCl(g) at 200 and 350°C in the presence of aluminum and zirconium respectively. The results indicate that enhanced volatility was observed for Sr, Sn, Mo, and Te in the presence of the cladding materials. Further experiments are recommended to assess the underlying phenomena and the relevance to processing SNF.

7. ACKNOWLEDGMENTS

The program was funded by DOE's Office of Nuclear Energy Nuclear Technology Research and Development Program, which is managed at ORNL by S. H. Bruffey. This manuscript was authored by UT-Battelle LLC, under contract DE-AC05-00OR22725 with DOE.

8. REFERENCES

Del Cul, G. D., Hunt, R. D. 2019. *Chlorination Scoping Tests on Aluminum 6061 Coupons*. ORNL/SPR-2019/1252. Oak Ridge: Oak Ridge National Laboratory.

Lawroski, S., Vögel, R. C., Munnecke, V. H. 1967. *Chemical Engineering Division, Summary Report, October, November, December 1967*. ANL-6477. Lemont: Argonne National Laboratory.

Lawroski, S., Vögel, R. C., Levenson, M., Munnecke, V. H. 1963. *Chemical Engineering Division, Summary Report January, February, March 1963*. ANL-6687. Lemont: Argonne National Laboratory .

McFarlane, J., Greaney, A. T., Hunt, R. D., Del Cul, G. D., Braatz, A. D. 2020. *Complete Al chlorination lab-scale testing with non-fuel materials*. ORNL/SPR-2020/1551. Oak Ridge: Oak Ridge National Laboratory.

McFarlane, J., Braatz, A. D., Birdwell, J. F. Jr., Bruffey, S. H., Del Cul, G. D., Greaney, A. T., Hunt, R. D., Ngelale, R. O., Taylor, P.A ., Walker, T. B. 2021. "Hydrochlorination at 200°C relevant to the removal of cladding from spent nuclear fuel." *Proceedings of the American Nuclear Society Annual Meeting* 124(1), 100–102.

APPENDIX A. ICP-MS RAW DATA

APPENDIX A. ICP-MS RAW DATA

Table A1. ICP-MS from initial digestion.

Analysis ID	Sample ID	Mass (g)	Type of sample	Units	Elements								
					Al	Sr	Zr	Mo	Sn	Te	Cs	La	I
1	Test 1 - Bed	0.3	Powder	µg/g	2.59E+02	6.36E+03	6.69E+00	2.00E+04	4.14E+01	1.52E+03	2.70E+04	6.01E+02	2.27E+02
2	Test 1 - Rxr Top	0.1	Powder	µg	6.42E+00	8.38E+02	1.25E+00	4.10E+03	4.86E+01	1.24E+02	6.73E+02	4.82E+01	1.79E+02
3	8-05-21-Reactor	49.4	Slurry in DI	µg	3.32E+00	2.56E+03	1.25E+00	1.09E+04	3.60E+02	1.75E+03	4.22E+03	3.71E+01	1.56E+03
4	8-05-21-1A	11.5	Slurry in DI	µg	6.70E+00	8.66E+01	2.27E+01	2.83E+03	4.37E+02	4.53E+02	1.01E+02	6.32E+01	1.55E+03
5	8-05-21-1B	31.0	Slurry in DI	µg	6.40E+00	8.55E+02	2.50E+00	4.59E+03	5.43E+02	1.84E+02	6.19E+02	3.39E+01	2.04E+03
6	Test 1 - scrubber	12.5	HCl	µg/ml	6.40E-02	2.40E-03	2.50E-02	4.13E+00	2.29E+00	2.49E+00	1.15E-01	1.36E-02	2.99E+01
7	Test 2 - Bed	1.7	Powder	µg/g	7.66E+03	6.18E+03	4.17E+01	9.93E+02	1.84E+02	5.55E+02	1.31E+04	2.36E+03	2.75E+02
8	Test 2 - Rxr Top	0.1	Powder	µg	1.08E+04	8.86E+02	8.49E+00	4.36E+03	1.14E+03	4.23E+01	2.44E+02	3.27E+02	3.22E+02
9	08-06-21-RxR Top	0.1	Powder	µg	1.43E+03	1.79E+02	1.46E+00	8.36E+02	2.28E+02	6.95E+00	4.98E+01	1.19E+02	7.27E+01
10	Test 2 - KOP	0.6	Powder	µg	9.93E+02	2.86E+03	1.25E+00	3.06E+04	2.30E+03	1.04E+02	1.03E+03	1.67E+02	3.26E+02
11	8-06-21-KOP-solid	0.2	Powder	µg	7.18E+01	2.89E+02	2.68E+00	4.19E+03	3.78E+02	1.35E+01	1.24E+02	8.68E+01	3.47E+01
12	8-06-21-RxR-Bed-Liq	32.6	Slurry in DI	µg	5.32E+05	3.38E+04	1.81E+03	1.70E+05	1.53E+04	4.28E+03	1.89E+05	5.65E+04	4.42E+03
13	8-06-21-RxR-Top-rinse	10.3	Slurry in DI	µg	5.61E+04	1.29E+03	8.84E+01	2.87E+04	2.25E+03	8.52E+01	6.73E+02	9.61E+02	9.37E+02
14	8-06-21-KOP-rinse	31.8	Slurry in DI	µg	5.91E+02	6.26E+03	2.60E+01	4.71E+04	1.82E+03	5.59E+02	3.08E+03	9.89E+02	1.24E+03
15	8-06-21-line-rinse	11.4	Slurry in DI	µg	4.19E+04	3.23E+04	2.50E+01	4.96E+05	3.73E+04	8.89E+03	2.74E+04	4.84E+02	6.95E+03

Table A1. ICP-MS from initial digestion (continued).

Analysis ID	Sample ID	Mass (g)	Type of sample	Units	Elements								
					Al	Sr	Zr	Mo	Sn	Te	Cs	La	I
16	Test 2 - scrubber	13.0	HCl	µg/ml	5.47E+00	1.37E-01	5.00E-01	2.44E+01	9.92E+00	1.95E-01	2.07E-01	3.67E-01	1.62E+01
17	8-16-21-RxR-top	0.1	Powder	µg/g	5.13E+02	9.18E+03	2.28E+05	6.53E+04	4.46E+03	5.09E+03	5.67E+03	2.44E+03	1.73E+03
18	8-16-21-KOP	1.5	Powder	µg/g	7.53E+02	1.17E+04	2.66E+05	9.06E+04	3.18E+03	1.34E+04	9.45E+03	2.66E+02	4.75E+03
19	8-16-21-RxR-Bed	41.6	Slurry in DI	µg	3.13E+03	1.01E+04	1.08E+05	1.82E+05	3.33E+03	9.81E+03	3.23E+04	2.56E+02	1.86E+03
20	8-16-21-RxR-top	5.0	Slurry in DI	µg	1.99E+02	1.65E+03	9.12E+03	4.22E+04	1.07E+03	1.84E+03	1.23E+03	5.18E+01	1.21E+03
21	8-16-21-transfer line	12.6	Slurry in DI	µg	7.20E+02	1.47E+04	3.45E+04	3.17E+05	9.28E+03	2.25E+04	1.37E+04	2.85E+03	4.28E+03
22	8-16-21-KOP	20.0	Slurry in DI	µg	2.94E+02	2.88E+03	9.79E+04	3.37E+04	2.36E+03	4.55E+03	2.76E+03	1.14E+03	2.39E+03
23	8-16-21-line out of KOP	8.0	Slurry in DI	µg/ml	1.45E+01	6.02E+00	1.07E+03	1.39E+03	3.30E+01	5.18E+01	2.67E+01	1.16E-01	4.90E+01
24	Test 3 - scrubber	13.8	HCl	µg/ml	2.54E+00	4.79E-02	1.39E+01	5.83E+00	1.36E+00	1.92E-01	1.18E-01	8.86E-02	9.76E+00

Table A2. Digestion and analysis of undissolved solids.

RMAL ID	210896-012		210896-014		210896-015		210896-019		210896-021		210896-022	
Metal	**µg/g**	**Uncert**	**µg/g**	**Uncert**	**µg/g**	**Uncert**	**µg/g**	**Uncert**	**µg/g**	**Uncert**	**µg/g**	**Uncert**
Al	2.32E+01	2.32E+00	< 2.49E+03		2.43E+03	2.43E+02	3.84E+03	3.84E+02	2.01E+03	4.02E+02	2.44E+02	2.44E+01
Sr	2.45E-01	4.90E-02	< 1.25E+02		3.04E+03	3.04E+02	6.13E+04	6.13E+03	3.14E+04	3.14E+03	1.60E+03	1.60E+02
Zr	1.28E+00	1.28E-01	7.78E+01	1.56E+01	1.79E+02	1.79E+01	7.15E+04	7.15E+03	4.79E+04	4.79E+03	3.73E+03	3.73E+02
Mo	< 1.38E+00		< 1.13E+03		1.02E+03	1.02E+02	4.15E+03	4.15E+02	1.13E+04	1.13E+03	1.17E+03	1.17E+02
Sn	2.61E-01	2.61E-02	9.98E+04	9.98E+03	7.34E+01	7.34E+00	1.17E+01	1.17E+00	1.56E+02	1.56E+01	3.92E+01	3.92E+00
Te	< 1.08E-01		8.28E+02	8.28E+01	2.36E+01	2.36E+00	2.92E+02	2.92E+01	2.58E+03	2.58E+02	1.14E+02	1.14E+01
Cs	1.87E-01	3.75E-02	2.33E+05	2.33E+04	7.69E+01	7.69E+00	4.62E+02	4.62E+01	3.17E+02	3.17E+01	3.23E+01	3.23E+00
La	2.99E+00	2.99E-01	7.71E+00	1.54E+00	1.23E+04	1.23E+03	4.94E+04	4.94E+03	4.92E+04	4.92E+03	9.14E+03	9.14E+02

Mass recovered (g)	0.0815	0.02598	-0.06134	0.02812	0.09662	0.01656
Mass digested (g)	0.06508	0.00794	0.00918	0.04818	0.10588	0.00660

RMAL ID	210896-012		210896-014		210896-015		210896-019		210896-021		210896-022	
Metal	**µg**	**Uncert**	**µg**	**Uncert**	**µg**	**Uncert**	**µg**	**Uncert**	**µg**	**Uncert**	**µg**	**Uncert**
Al	1.51E+00	1.51E-01	< 1.97E+01		2.23E+01	2.23E+00	1.85E+02	1.85E+01	2.13E+02	4.26E+01	1.61E+00	1.61E-01
Sr	1.60E-02	3.19E-03	< 9.94E-01		2.79E+01	2.79E+00	2.95E+03	2.95E+02	3.33E+03	3.33E+02	1.06E+01	1.06E+00
Zr	8.30E-02	8.30E-03	6.18E-01	1.24E-01	1.64E+00	1.64E-01	3.44E+03	3.44E+02	5.07E+03	5.07E+02	2.46E+01	2.46E+00
Mo	< 8.97E-02		< 8.97E+00		9.39E+00	9.39E-01	2.00E+02	2.00E+01	1.20E+03	1.20E+02	7.75E+00	7.75E-01
Sn	1.70E-02	1.70E-03	7.93E+02	7.93E+01	6.74E-01	6.74E-02	5.63E-01	5.63E-02	1.65E+01	1.65E+00	2.59E-01	2.59E-02
Te	< 7.04E-03		6.57E+00	6.57E-01	2.17E-01	2.17E-02	1.41E+01	1.41E+00	2.73E+02	2.73E+01	7.52E-01	7.52E-02
Cs	1.22E-02	2.44E-03	1.85E+03	1.85E+02	7.06E-01	7.06E-02	2.23E+01	2.23E+00	3.35E+01	3.35E+00	2.13E-01	2.13E-02
La	1.95E-01	1.95E-02	6.13E-02	1.23E-02	1.13E+02	1.13E+01	2.38E+03	2.38E+02	5.21E+03	5.21E+02	6.03E+01	6.03E+00